Supplementary Information

List of supplementary information:

Table S7 Degradation intermediate

Text S1 Determination of iron ion concentration

The iron ion concentration in the solution was determined by o-phenanthroline chromogenic method. Ferrous ion could form a red complex with colorless phenanthroline. The complex had a strong characteristic absorption peak at 510 nm, which could be detected by UV spectrophotometer. When determining the concentration of Fe^{2+} or total iron ion, 0.5 mL hydrochloric acid amine solution (100 mg/L) or water was added to 0.5 mL sample to be tested, then 0.5 mL phenanthroline solution (1 g/L) and 0.5 mL sodium acetate solution (mass fraction 10%) were added. Then the solution was shaken evenly for color development and the absorbance of the sample was determined.

Text S2 LC-MS Analysis

The intermediates were isolated using an ACQUITY UPLC® BEH C18 column (2.1 × 50 mm, 1.7 μm). A mobile phase including formic acid (A) and acetonitrile (B) was used. Sample Cone: 30-60 V; Extraction Cone: 30-60 V; Source temperature: 120 °C; Desolvation temperature: 350 °C; Cone Gas: 50 L/h; Desolvation Gas: 800 L/h. According to the mass-to-charge (*m/z*) value, the LC-MS chromatogram of the intermediate product of MO degradation was shown in Fig. S7.

Text S3 Energy efficiency

In order to quantitatively evaluate the energy efficiency under different systems, the conversion rate per unit time per unit current was calculated according to Equation (S1-1), which was expressed as *EE* ($A^{-1}min^{-1}$):

$$EE = \frac{d_r}{I \times t} \tag{S1-1}$$

Where I (A) was the current, t (min) was the degradation time, d_r (%) was final degradation rate, and EE ($A^{-1}min^{-1}$) was energy efficiency.

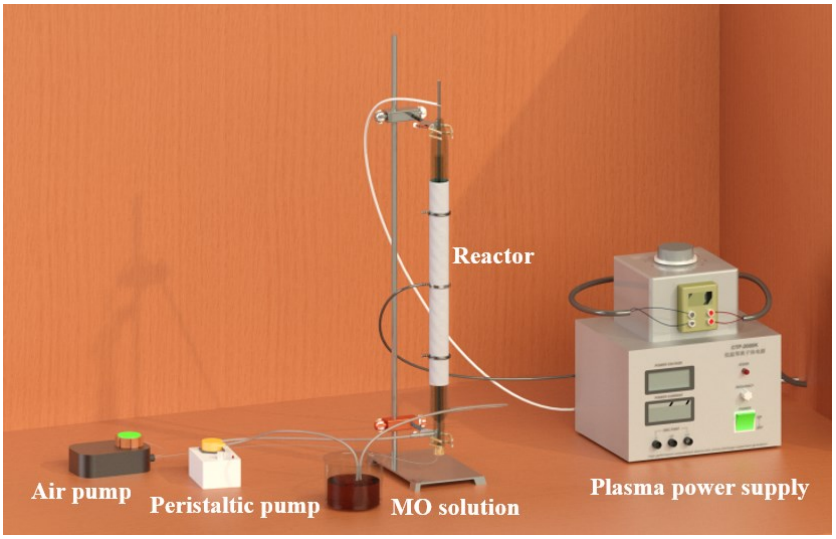

Fig. S1 Degradation experimental device diagram.

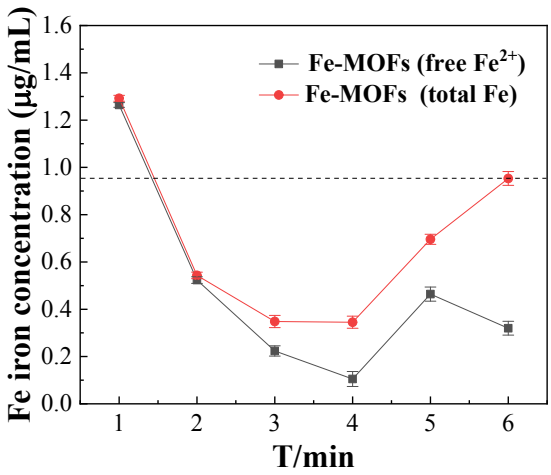

Fig. S2 Determination of Fe ion concentration in sample reaction process.

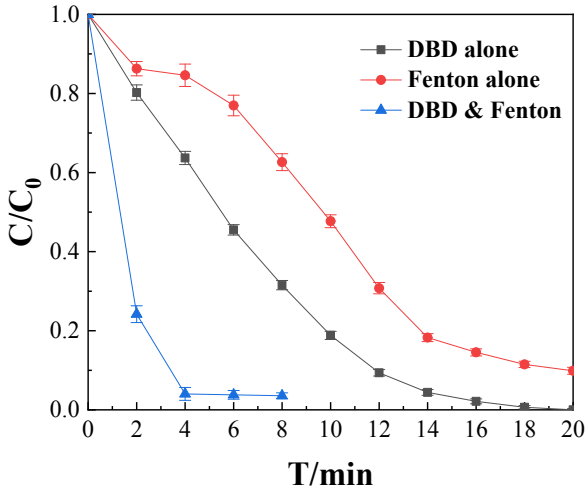

Fig. S3 Comparison of the performance with different methods.

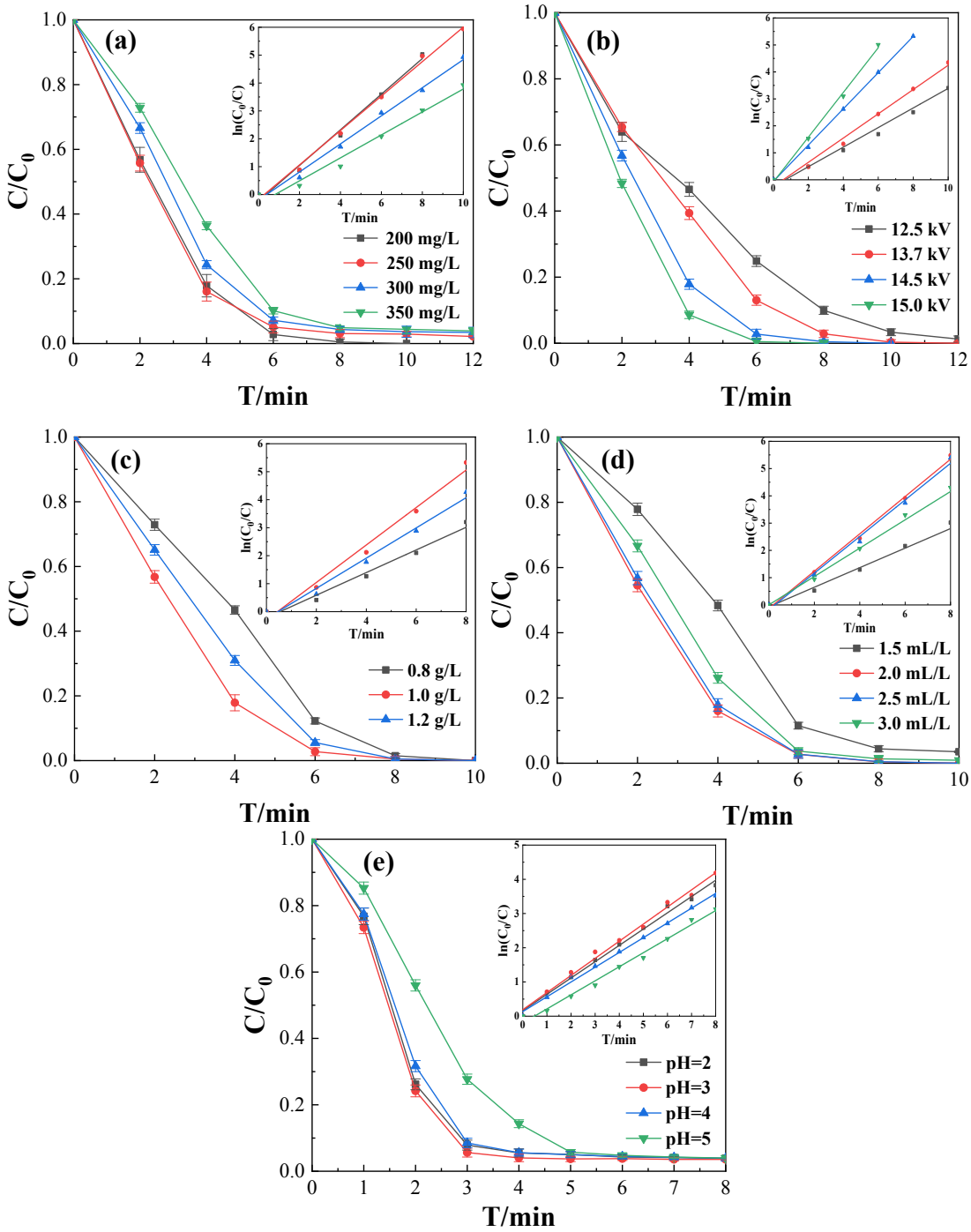

Fig. S4 Effect of different reaction conditions on performance of Fe-MOFs (a) MO concentration; (b) discharge voltage; (c) catalyst addition amount; (d) H_2O_2 addition amount; (e) pH.

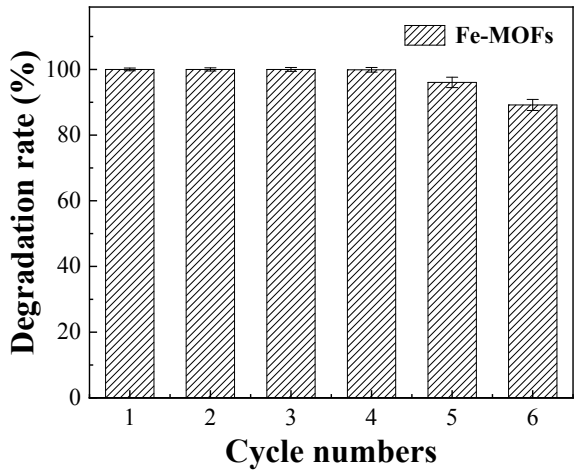

Fig. S5 Recyclability and reusability tests.

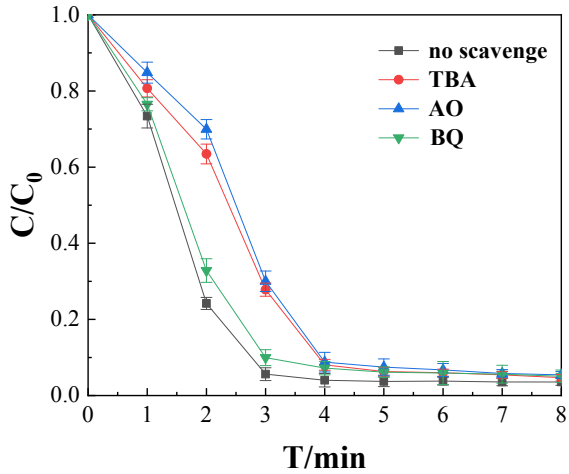

Fig. S6 Effect of capture agents on MO degradation during plasma/Fenton-like process.

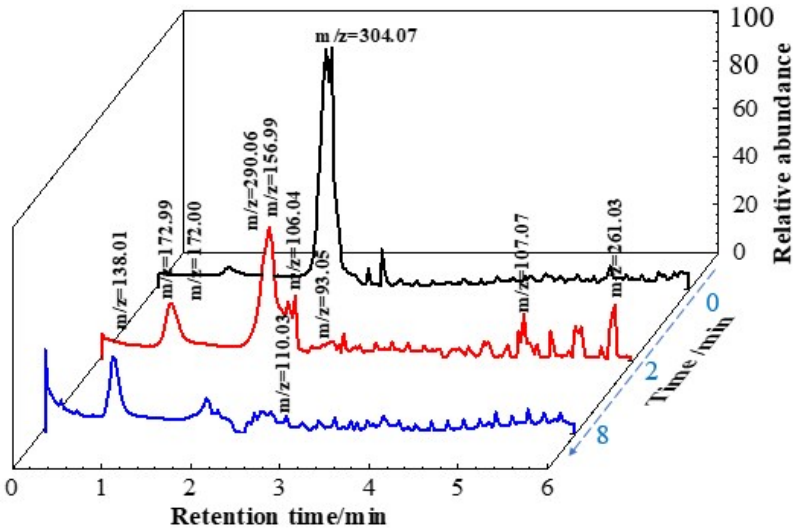

Fig. S7 LC-MS chromatograms corresponding to the intermediates of MO degradation.

Table S1 Average particle size of Fe-MOFs with different TA/Fe molar ratios

TA/Fe molar ratio	Average particle size /(nm)
1: 1	49
1: 2	24
1: 3	17
1: 4	23

Table S2 Composition of Fe-MOFs with different TA/Fe molar ratios

TA/Fe molar ratio	EDS wt%	
	Fe	O
1: 1	24.19	75.81
1: 2	32.61	67.39
1: 3	43.39	56.61
1: 4	28.31	71.69

Table S3 Surface and pore structure of Fe-MOFs with different TA/Fe molar ratios

TA/Fe molar ratio	Surface area ($m^2 \cdot g^{-1}$)	Average pore size (nm)	Pore volume ($cm^3 \cdot g^{-1}$)
1: 1	3.123	3.816	0.007
1: 2	20.864	3.411	0.154
1: 3	32.021	17.186	0.210
1: 4	19.992	3.410	0.131

Table S4 Binding energies of Fe2p, O1s, and C1s for Fe-MOFs

TA/Fe molar ratio	Binding energy /(eV)									
	Fe 2p					C1s			O1s	
	Fe^{2+} $2p_{3/2}$	Fe^{3+} $2p_{3/2}$	satellite peak	Fe^{2+} $2p_{1/2}$	Fe^{3+} $2p_{1/2}$	C1s A	C1s	C1s B	O1s	O1s A
1: 1	711.17	712.94	717.02	724.48	726.46	284.54	285.34	288.91	531.44	532.18
1: 2	711.40	713.36	717.51	724.81	726.74	284.72	285.73	288.67	531.25	531.97
1: 3	711.11	712.72	716.18	724.47	726.10	284.68	285.61	288.64	531.24	532.00
1: 4	711.08	712.49	715.59	724.01	726.00	284.70	285.80	288.64	531.31	532.09

Table S5 Proportion of different valence elements of Fe-MOFs with different TA/Fe molar ratios

TA/Fe molar ratio	Proportion /(%)			
	Fe^{2+}	Fe^{3+}	Fe^{2+}/Fe^{3+}	$[O]_s/([O]_l+[O]_s)$
1: 1	46.85	45.36	1.03	42.89
1: 2	43.21	38.22	1.13	43.96
1: 3	46.83	39.94	1.17	44.00
1: 4	42.27	46.85	0.90	42.61

Table S6 Comparison of degradation ability by different systems

systems	catalyst	pollutants	pH	pollutants concentration (mg/L)	pollutants treatment capacity (mL)	catalyst addition amount (g/L)	Reaction time (min)	Degradation rate (d_r) (%)	EE ($A^{-1}min^{-1}$)	References
DBD plasma/Fenton-like	Fe-MOFs	MO	3	200	200	1.0	8	96.4	8.03	This work
PDP/Fenton	$FeSO_4 \cdot 7H_2O$	Bisphenol A	5.5	4.566	600	2.0	30	97	2.16	[11]
GAD/Fenton	ZVI (Fe^0)	Acid Orange 7	7.4	63	400	26	25	80	0.64	[13]
Electro Fenton	pyrite	tyrosol	3	41	250	1.0	60	96	5.33	[38]
Electro Fenton	$FeSO_4 \cdot 7H_2O$	chloroquine drug	3	125	400	0.01	300	100	5.56	[39]
Electro Fenton	iron plate electrode	diisobutyl phthalate	4	10	500	-	45	93	2.07	[40]

Table S7 Degradation intermediate

Relative molecular mass	Structure
304.07	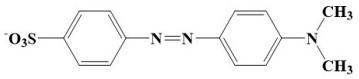
290.06	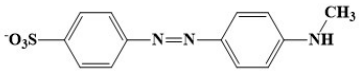
261.03	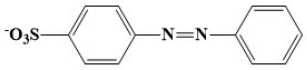
172.99	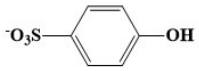
172.00	
156.99	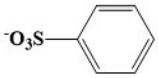
138.01	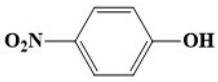
110.03	
107.07	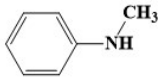
106.04	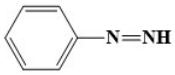
93.05	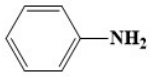

References

11. F. Dai, X.R. Fan, G.R. Stratton, C.L. Bellona, T.M. Holsen, B.S. Crimmins, X.Y. Xia, S.M. Thagard, *J. Hazard. Mater.* 2016, 308, 419-429. https://doi.org/10.1016/j.jhazmat.2016.01.068.

13. C.M. Du, L.L. Zhang, J. Wang, C.R. Zhang, H.X. Li, Y. Xiong, *Plasma Chem. Plasma P.* 2010, 30, 855-871. https://doi.org/10.1007/s11090-010-9249-0.

38. S. Ammar, M.A. Oturan, L. Labiadh, A. Guersalli, R. Abdelhedi, N. Oturan, E. Brillas, *Water Res.*, 2015, 74, 77-87. http://dx.doi.org/10.1016/j.watres.2015.02.006.

39. S. Midassi, A. Bedoui, N. Bensalah, *Chemosphere.*, 2020, 260, 127558. https://doi.org/10.1016/j.chemosphere.2020.127558.

40. Z.Q. Yang, H.L. Chen, J.H. Wang, Q.F. Yuan, F. Wang, B.H. Zhou, *J. Environ. Chem. Eng.*, 2020, 8, 104057. https://doi.org/10.1016/j.jece.2020.104057.